Session 6

Coronal mass ejections and energetic particles

Magnetic Field $\vec{B}$
Mean Field $\langle \vec{B} \rangle$
Particle Motion
Solar Wind
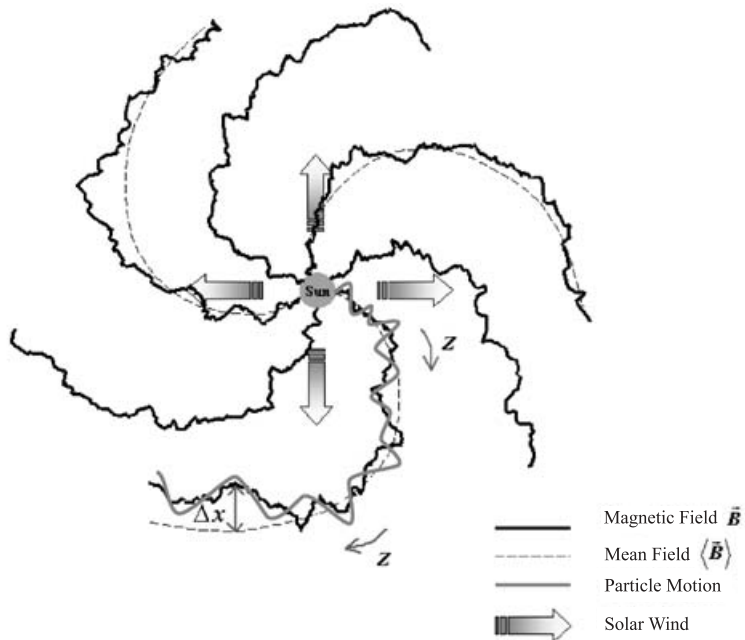
Transport and Acceleration of Solar Energetic Particles from Coronal Mass Ejection Shocks

David Ruffolo

Dept. of Physics, Faculty of Science, Mahidol Univ., Bangkok 10400 Thailand,
email: david_ruffolo@yahoo.com

Abstract. After a brief overview of solar energetic particle (SEP) emission from coronal mass ejection (CME) shocks, we turn to a discussion of their transport and acceleration. The high energy SEP are accelerated near the Sun, and because of their well-known source location, their transport can be modeled quantitatively to obtain precise information on the injection function (number of particles emitted vs. time), including a determination of the onset time to within 1 min. For certain events, transport modeling also indicates magnetic topology with mirroring or closed field loops. Important progress has also been made on the transport of low energy SEP from very strong events, which can display exhibit interesting saturation effects and compositional variations. The acceleration of SEP by CME-driven shocks in the interplanetary medium is attributed to diffusive shock acceleration, but the spectrum of SEP production is typically modeled empirically. Recent progress has largely focused on using detailed composition measurements to determine fractionation effects of shock acceleration and even to clarify the nature of the seed population. In particular, there are many indications that the seed population is suprathermal (pre-energized) and the injection problem is not relevant to acceleration at interplanetary CME-driven shocks. We argue that the finite time available for shock acceleration provides the best explanation of the high-energy rollover.

Keywords. Sun: particle emission — Sun: coronal mass ejections (CMEs) — interplanetary medium — solar-terrestrial relations

1. Overview of solar energetic particle transport

This presentation aims to provide a brief introduction to the basic issues and some appreciation of state of the art in solar energetic particle (SEP) transport and acceleration, for a broad audience of specialists in different aspects of coronal mass ejections (CMEs).

Figure 1 shows the first report, in 1962, of energetic particles associated with an interplanetary shock, which we now believe to be driven by a CME (Bryant, Cline, Desai, *et al.* 1962). This shows the flux of protons in different energy ranges as a function of time. There are evidently two distinct populations. The first arrives shortly after the time of the flare [which we now know to be closely related to the time of CME liftoff; see Zhang *et al.* (2004)]. While the CME and shock were still very close to the Sun, protons were accelerated to several hundred MeV. On a finer timescale, SEP of higher velocity are seen to arrive first; this is termed a dispersive onset. On the other hand, there is a delayed, non-dispersive peak that dominates at low energies, associated with shock passage by the observer (in this case near Earth, as identified by a sudden storm commencement, SC). This evidently corresponds to particles accelerated by the shock as it proceeds through the interplanetary medium. These have been termed "energetic storm particles," although in recent usage both these and prompt population are referred to collectively as solar energetic particles, because at lower energies the two populations are

not cleanly separated. Finally, Figure 1 shows the response of a ground-based neutron monitor, which measures the flux of galactic cosmic rays (GCR) impacting the atmosphere from a specific direction in space (by means of secondary atmospheric neutrons). Interestingly, the flux of GCR is depressed when a shock passes the Earth and sweeps these particles away. This phenomenon is known as a Forbush decrease (Forbush 1937). However, a very strong event can produce SEP to GeV energies and register an increase in neutron monitor rates; such a event is called a ground level enhancement (GLE).

(a) (b)
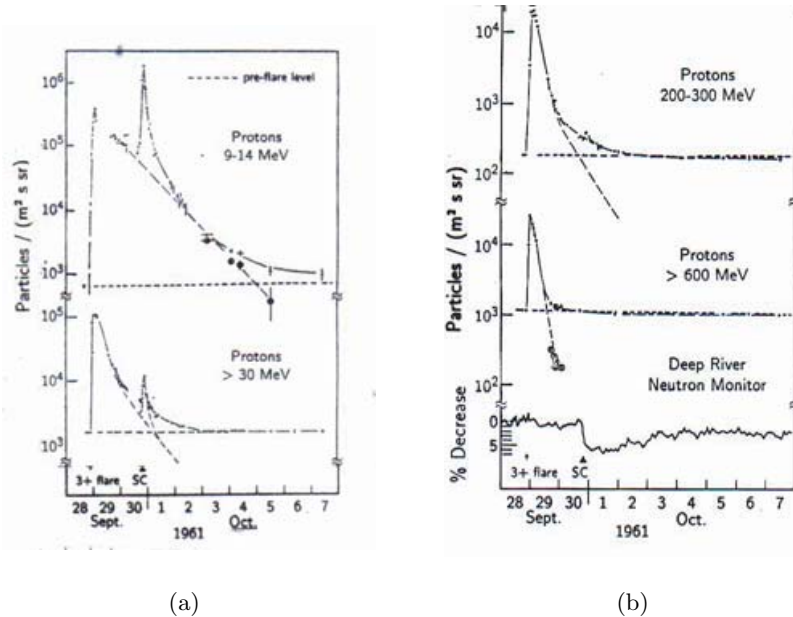
Figure 1. Representative proton intensities between September 28 and October 7, 1961; the decay of the solar proton event and the arrival of the energetic storm particles late on September 30 are shown. The Deep River neutron monitor record is shown for comparison. [Based on Fig. 18 of Bryant *et al.* (1962)]

There is now overwhelming physical evidence that for the class of "gradual" events that have a solar flare and a coronal mass ejection (including the geoeffective events with greatest SEP intensity), the escaping SEP are accelerated at the CME shock and not deep in the corona, e.g., not at the site of the flare or primary energy release (Mason, Gloeckler, & Hovestadt 1984; Lee & Ryan 1986; Reames 1990; Ruffolo 1997). Therefore, the two populations shown in Figure 1, with very different energy spectra, both correspond to shock acceleration, but under very different physical conditions while the shock is still close to the Sun and later as it moves in the interplanetary medium.

I would like to comment that discussions of geoeffectiveness typically stress the effects when a CME and its associated shock impact the Earth's magnetosphere, which is typically days after its liftoff from the Sun. For example, the largest SEP event of 2003 had a flare and CME on October 28 and the CME arrived at Earth on October 29. However, in a recent presentation, a NASA representative stated that more satellite anomalies occurred on October 28 than on October 29 (L. Barbieri, private communication, 2004). Therefore, the flare/CME at the Sun is immediately geoeffective in the sense of producing prompt space weather effects.

The main types of SEP populations are summarized in Table 1. In addition to the gradual events we have discussed so far, associated with a CME (and for major events, a flare as well), another type of event is an impulsive solar flare, with no associated CME. In this case the energetic particles are believed to result from stochastic acceleration, and there are very interesting compositional effects, such as enhancements in the isotope ^{3}He (Hsieh & Simpson 1970) and heavy ions (Hurford, Mewaldt, Stone, *et al.* 1975; Reames 2000) by factors up to 10^3 or even 10^4, an enhancement in electrons (Evenson, Meyer, Yanagita, *et al.* 1984; Cane, McGuire, & von Rosenvinge 1986), and high charge states (Klecker, Hovestadt, Gloeckler, *et al.* 1984; Luhn, Klecker, Hovestadt, *et al.* 1987).

Table 1. Populations of escaping solar energetic particles

Impulsive flares	CME shocks (gradual events)	
	Near Sun	Interplanetary
^{3}He enhanced, electron-rich, high ion Q (stochastic acceleration)	Up to high E dispersive onset	At low E non-dispersive
	(shock acceleration)	

2. Injection near the Sun: Precision modeling

According to Figure 1 and Table 1, SEP at high energy are almost always injected near the Sun. With this well-determined source, and given that the basic transport processes are well established, we are able to undertake precision modeling to determine transport parameters, the magnetic field configuration in space, and the injection vs. time near the Sun. We discuss transport of the interplanetary component in §4.

We describe the propagation of protons from a solar event by numerically solving a Fokker-Planck equation of pitch-angle transport that includes the effects of interplanetary scattering, adiabatic deceleration and solar wind convection (Roelof 1969; Ruffolo 1995; Nutaro, Riyavong, & Ruffolo 2001). We are assuming transport along the mean magnetic field, as expected when there is good magnetic connection between the source and the observer. Following Ng & Wong (1979), we define the particle distribution function F depending on time, t, pitch-angle cosine, μ, distance from the Sun along the interplanetary magnetic field, z, and momentum, p, as

$$F(t, \mu, z, p) \equiv \frac{d^3 N}{dz \, d\mu \, dp}, \tag{2.1}$$

where N represents the number of particles inside a given flux tube. The derived transport equation takes the form:

$$\begin{aligned}
\frac{\partial F(t, \mu, z, p)}{\partial t} = &- \frac{\partial}{\partial z} \mu v F(t, \mu, z, p) - \frac{\partial}{\partial z} \left(1 - \mu^2 \frac{v^2}{c^2} \right) v_{\text{sw}} \sec \psi F(t, \mu, z, p) \\
&- \frac{\partial}{\partial \mu} \frac{v}{2L(z)} \left[1 + \mu \frac{v_{\text{sw}}}{v} \sec \psi - \mu \frac{v_{\text{sw}} v}{c^2} \sec \psi \right] (1 - \mu^2) F(t, \mu, z, p) \\
&+ \frac{\partial}{\partial \mu} v_{\text{sw}} \left(\cos \psi \frac{d}{dr} \sec \psi \right) \mu(1 - \mu^2) F(t, \mu, z, p) \\
&+ \frac{\partial}{\partial \mu} \frac{\varphi(\mu)}{2} \frac{\partial}{\partial \mu} \left(1 - \mu \frac{v_{\text{sw}} v}{c^2} \sec \psi \right) F(t, \mu, z, p) \\
&+ \frac{\partial}{\partial p} p v_{\text{sw}} \left[\frac{\sec \psi}{2L(z)} (1 - \mu^2) + \cos \psi \frac{d}{dr} (\sec \psi) \mu^2 \right] F(t, \mu, z, p). \tag{2.2}
\end{aligned}$$

The particle velocity is denoted by v and the solar wind velocity by v_{sw}. The angle between the field line and the radial direction is specified by the function $\psi(z)$, the focusing length by $L(z) = -B/(dB/dz)$, and the pitch-angle scattering coefficient by $\varphi(\mu)$. The simulation program to solve this equation runs in a few minutes on a personal computer.

In the next step, we can simultaneously fit observed data for the SEP intensity and anisotropy vs. time. It is computationally efficient to use least squares fitting to determine the optimal piecewise linear injection function, i.e., the rate of particle injection onto the local magnetic field line vs. time near the Sun (Ruffolo, Khumlumlert, & Youngdee 1998). We find the χ^2 values of fits for different transport assumptions to determine the optimal model. For a standard Archimedean spiral field configuration (Figure 2), typically the only parameter we vary is the interplanetary scattering mean free path. Note that anisotropy data are important for constraining the optimal scattering mean free path.

————	Magnetic Field $\vec{B}$
- - - - -	Mean Field $\langle \vec{B} \rangle$
————	Particle Motion
▯▯▭⟩	Solar Wind
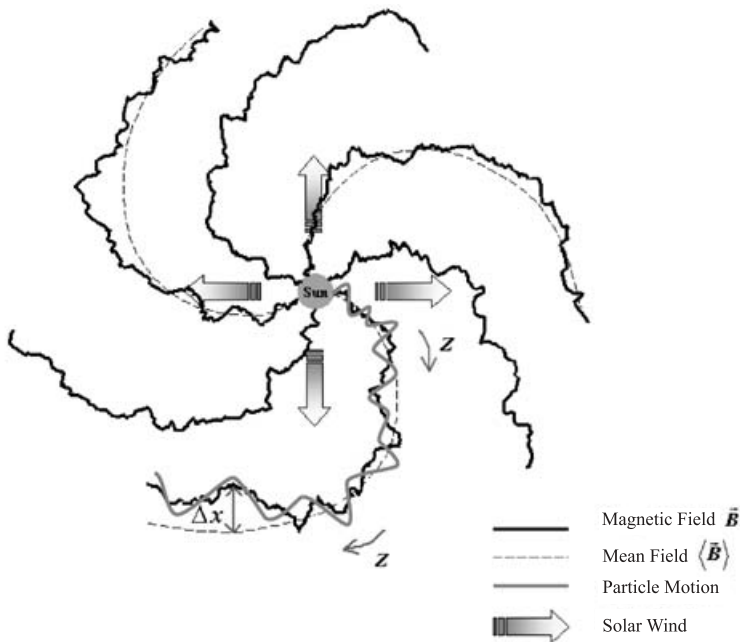
Figure 2. Typical Archimedean spiral configuration of the interplanetary magnetic field as it is dragged out of the rotating Sun by the radial solar wind.

An example of such precision modeling for the GLE of 2001 April 15 (Easter 2001) is shown in Figure 3. The intensity and anisotropy of relativistic solar protons (at rigidity ∼1-3 GV) are derived from count rate increases in the *Spaceship Earth* network of polar neutron monitors, which provide high count rates and excellent directional sensitivity, and the data are then fit by the above procedure. The injection function is interpreted as the time profile of relativistic particle acceleration. Table 2 compares the injection timing with electromagnetic emissions converted into "solar time," ST, or UT minus 8 minutes to account for the propagation time. It is of particular interest that the start time of relativistic particle acceleration is coincident with the soft X-ray peak, which
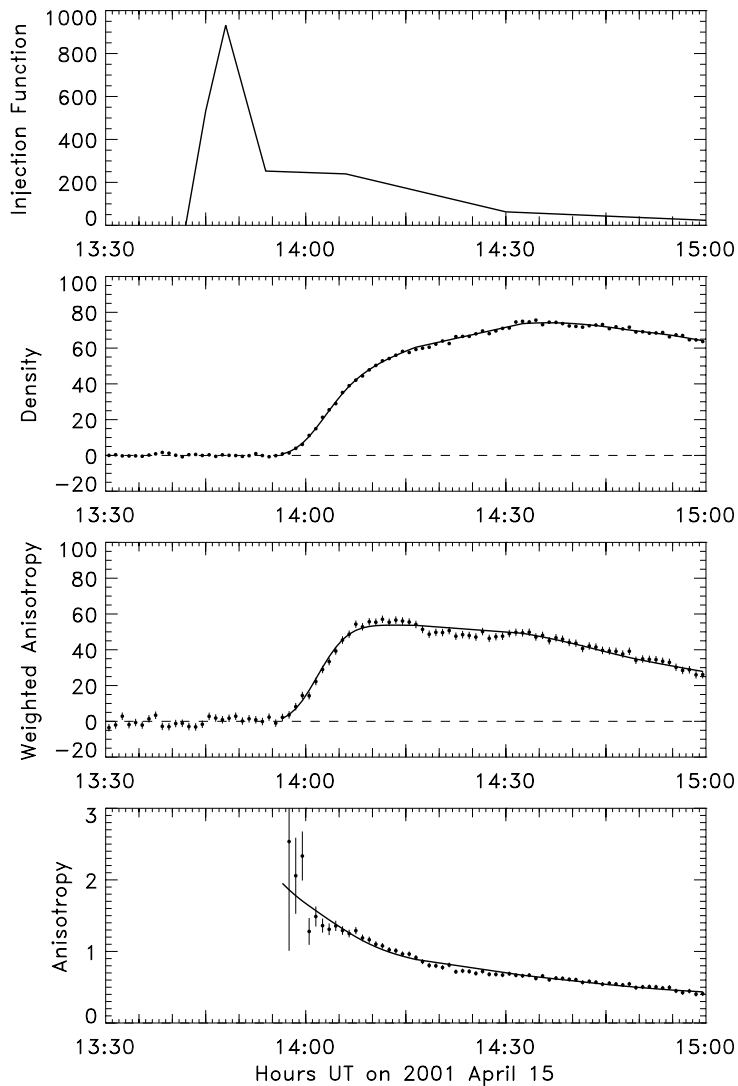
Figure 3. Precision modeling of relativistic solar proton data from neutron monitors on Easter, 2001 [Bieber, Evenson, Dröge, *et al.* (2004)].

actually marks the end of energy input in the flare. It is also later than the extrapolated CME liftoff time. Our interpretation is that the CME shock takes some time to develop and accelerate relativistic particles. Nevertheless, it does occur quite quickly; the time of relativistic particle injection corresponds to a CME altitude of only a few solar radii (Cliver, Kahler, & Reames 2004).

In some cases, such detailed fitting allows us to infer a non-standard magnetic field configuration. For example, in the GLE of 2000 July 14 (Bastille Day 2000), Bieber, Dröge, Evenson, *et al.* (2002) inferred a magnetic bottleneck configuration as in Figure 4. This corresponds to distortion of interplanetary magnetic field lines beyond the Earth by a preceding CME from the same active region a few days earlier. This is not as unusual as you might think, because major flare/CME events typically occur in sequences a few

Table 2. Timing of flare, CME, and particle emission on Easter, 2001 [Bieber *et al.* (2004)], in "solar time" (see text).

Emission	2001 April 15		
	Start	Peak	End
Relativistic protons	**13:42**	**13:48**	
Soft X-rays	13:11	13:42	13:47
Hα	13:28	13:41	15:27
Type III radio burst	13:36		13:38
CME liftoff	13:24-31		
Type II radio burst	13:40		13:47
Type IV radio burst	13:44		14:57
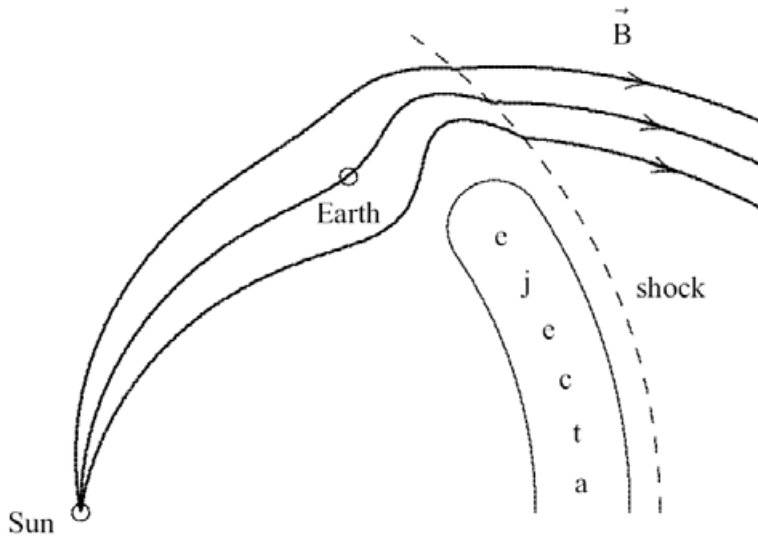
Figure 4. Magnetic bottleneck configuration inferred at the time of the Bastille Day, 2000 GLE [Bieber *et al.* (2002)].

days apart from the same active region. Indeed for two other GLEs we infer from the angular distributions that relativistic solar protons were propagating inside a magnetic loop configuration (Ruffolo, Tooprakai, Rujiwarodom, *et al.* 2004; Bieber, Clem, Evenson, *et al.* 2005). This important information about particle transport again relies on accurate measurements of directional distributions of SEP, such as those from the worldwide neutron monitor network or from rotating spacecraft with multiple sensor heads.

3. Transport perpendicular to the mean magnetic field

So far we have discussed SEP transport parallel to the mean magnetic field, commonly called "parallel transport." Another important issue is perpendicular transport, i.e., perpendicular to the mean magnetic field, which governs the latitudinal and longitudinal transport of SEP. In the classic work of Jokipii (1966), such transport is considered to be dominated by the field line random walk. As illustrated in Figure 2, the interplanetary magnetic field fluctuates strongly due to solar wind turbulence, and individual field lines can undergo a random walk that deviates quite far from the mean magnetic field. This was classically viewed as a diffusive random walk, and one can define a field line diffusion coefficient in terms of the lateral deviation Δx compared with the distance along the

mean field, Δz:

$$\text{field line diffusion} \quad \rightarrow \quad D = \frac{\langle \Delta x^2 \rangle}{2\Delta z}. \tag{3.1}$$

The field line diffusion is related to the particle diffusion coefficient:

$$\text{particle diffusion} \quad \rightarrow \quad \kappa = \frac{\langle \Delta x^2 \rangle}{2\Delta t}, \tag{3.2}$$

and in the limit that particles exactly follow the field lines, one obtains $\kappa = Dv/4$.

For a realistic model of solar wind turbulence, Matthaeus, Gray, Pontius, *et al.* (1995) derived an expression for D, and Bieber & Matthaeus (1997) developed a theory for κ based on concepts of dynamical turbulence. Giacalone & Jokipii (1999) used Monte Carlo simulations to derive κ values intermediate to those for the classic field line random walk model and for dynamical turbulence. Recently, Qin, Matthaeus, & Bieber (2002) and Matthaeus, Qin, Bieber *et al.* employed numerical simulations and a nonlinear guiding center theory to show that in the ensemble average, particles undergo diffusion, then subdiffusion (also known as compound diffusion), and finally a second régime of diffusion at a slower rate.

Interestingly, Mazur, Mason, Dwyer *et al.* (2000) presented observations of SEP from impulsive flares (which are particle sources of narrow lateral extent) with "dropouts" or sudden disappearance and reappearance of flux as a function of time, which is interpreted as due to the spacecraft's motion through a filamentary distribution of magnetic flux tubes, of typical width 0.03 AU, that are filled with particles because they connect back to the source region. This shows that the lateral transport of SEP, and presumably the field lines themselves, is highly non-diffusive over a distance scale of 1 AU. To address this, Ruffolo, Matthaeus, & Chuychai (2003) replaced ensemble statistics with conditional statistics dependent on the starting point. For a standard description of solar wind turbulence, with no free parameters, they were able to simultaneously reproduce dropout structures of field lines at 1 AU connected to a small initial region and also explain the high rate of lateral diffusion κ inferred from observations by the Ulysses spacecraft (McKibben, Lopate, & Zhang 2001). The resulting picture (Figure 5) is that field lines starting near O-points in the turbulence are topologically trapped for some distance beyond 1 AU, whereas other field lines escape very rapidly. This accounts for a "core" region of outgoing SEP, with dropouts, and the SEP missing from the interstitial core regions are instead in a "halo" of low SEP density over a wide lateral region. At long radial distances all the field lines are found to escape and undergo diffusive random walks, so that particles undergo parallel and perpendicular diffusion throughout the inner heliosphere at later times.

4. Particle acceleration by coronal mass ejection shocks in the interplanetary medium

Referring to Table 1, we now turn to SEP accelerated by CME shocks traveling through the interplanetary medium (also referred to as energetic storm particles). We are fortunate to have other presenters who will show detailed results about these particles, so I will present only a broad-brush overview to help orient the non-specialist reader. While such SEP are certainly important, and also relevant to space weather effects, the underlying processes of acceleration and transport are poorly understood because they are both time-dependent and difficult to separate. (We saw in Section 1 that when acceleration and transport can be considered individually, the observations can clearly address each
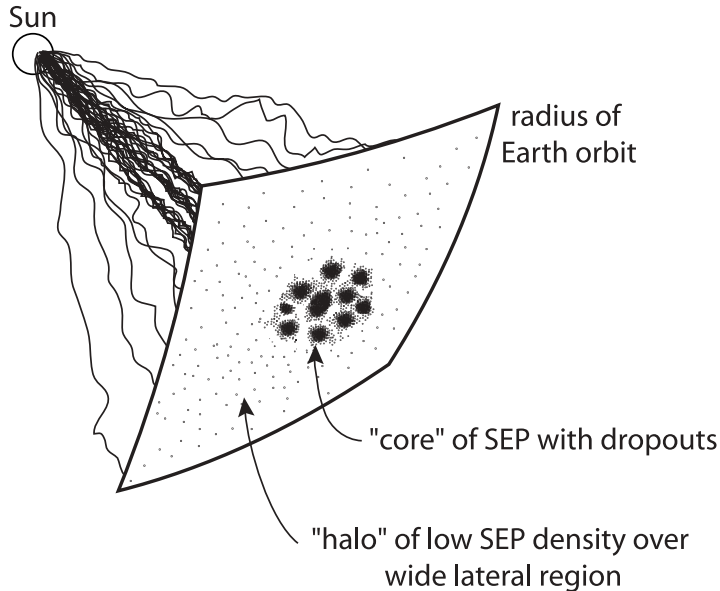
Figure 5. Illustration of the temporary trapping of magnetic field lines due to the small scale topology of solar wind turbulence [Ruffolo *et al.* 2003]. Trapped field lines form a core region with high SEP density and dropouts, while escaping field lines form a wider halo of lower SEP density. At long distances the field lines and particles ultimately escape to participate in diffusive random walks.

of them.) Modeling the simultaneous acceleration and transport of particles in the time-dependent system of a CME, shock, magnetic field topology, and magnetic fluctuations (the last of which are also affected by the particles) is necessarily difficult and involves many simplifying assumptions that are not well constrained by observations. Because of the complicated time dependence, recent research has concentrated on variations in ionic composition to probe the underlying physical processes.

That said, there have been important improvements in understanding. In a series of papers, Ng and others have examined saturation effects in very intense SEP events, based on the idea that the particles generate waves that in turn enhance interplanetary scattering and inhibit their transport. Ng, Reames, & Tylka (1999) provided a remarkable explanation of observed changes in element ratios as a function of time, confirming that wave generation probably plays a major role in these very intense events. However, other predictions of the theory, such as very intense waves and extremely low scattering mean free paths (below 10^{-3} AU) have not been confirmed by observations.

Before proceeding further, let me present a simple introduction to the process of diffusive shock acceleration. Figure 6 is a schematic of a shock, i.e., a discontinuity in fluid properties caused by a collision between fluids (or a fluid and an obstacle) with a relative speed greater the speed of sound. In general, the magnetic field (slanted lines in Figure 6) also has a different direction on the upstream and downstream sides. Usually we can enter a reference frame in which the fluid flow $\vec{u}$ is along $\vec{B}$ both upstream and downstream, called the de Hoffmann-Teller frame (de Hoffmann & Teller 1950). As the microscopic particle scatters off the ubiquitous macroscopic magnetic irregularities flowing with speed u in the space plasma, it is analogous to a game our Chinese audience knows and loves: ping-pong. If you hit the ping-pong ball with your paddle moving forward, the ball is

accelerated. This is what we see occurring on the upstream side, after the head-on collision. However, if you imagine moving your paddle backwards (not that a good Chinese ping-pong player would ever do this), the ball loses energy. This is analogous to the particle's deceleration on the downstream side. However, a shock always has $u_1 > u_2$, so there is always a net gain in energy after a complete cycle. The particle has some probability of crossing and recrossing the shock plane, and a small number of particles can achieve a very high energy. Indeed, the number of particles per unit momentum, which we call the spectrum, is a power law for standard theories of diffusive shock acceleration (Drury 1983).
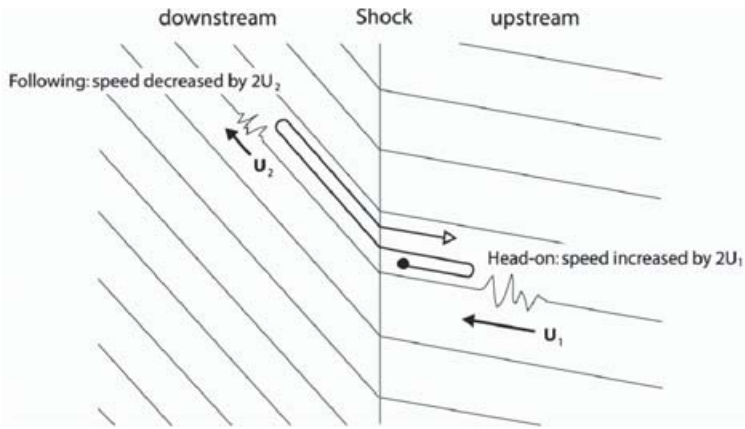
Figure 6. Illustration of diffusive shock acceleration as a particle scatters off magnetic irregularities, crossing and recrossing a shock discontinuity.

Figure 6 shows how an energetic seed particle can gain further energy at a shock. Until recently, interplanetary shocks were generally believed to accelerate particles out of the thermal solar wind population. However, there is a theoretical difficulty in understanding how thermal particles can join the shock acceleration process, the so-called "injection problem." Quite recently, Desai, Mason, Dwyer, *et al.* (2003) have analyzed the elemental composition of energetic storm particles to infer that those SEP were accelerated from a seed population of suprathermal (pre-energized) particles that happen to be upstream of the shock. Perhaps these were remnants from previous SEP events. Therefore, the injection problem is not relevant to acceleration at interplanetary CME-driven shocks.

Desai, Mason, Wiedenbeck, *et al.* (2004) have also examined the energy spectra of both the energetic storm particles and their upstream seed populations. The spectra are examined at the time of shock passage, which is one way to isolate the issue of acceleration from that of transport. They confirm a well-known rollover in the spectrum at 0.1-10 MeV nucleon^{-1} (see also Gosling, Asbridge, Bame, *et al.* 1981; van Nes, Reinhard, Sanderson, *et al.* 1985), where the power-law spectrum in particle energy changes to decline more rapidly above a critical energy, T_c. Such spectra are typically modeled empirically using the spectral form of Ellison & Ramaty (1985) for T_c as a fit parameter. However, this limit to the acceleration process is an important component of our understanding of SEP acceleration, and should be understood physically. Indeed, the critical energy must be higher near the Sun as the more energetic SEP originate there (see Table 1).

Of the possible rollover mechanisms listed by Ellison & Ramaty (1985) that might explain the rollover at 0.1-10 MeV nucleon^{-1} in the spectrum of particles accelerated by a CME-driven shock in the interplanetary medium, Ruffolo & Channok (2003) argue that

the rollover is due to the finite time available for shock acceleration (see also Klecker, Scholer, Hovestadt, *et al.* 1981; Lee 1983). This allows one to derive spectra for various ionic species in terms of the physical quantities that underlie the acceleration time. For a rollover energy well above the initial energy of the seed particle, and if the mean free path λ is proportional to rigidity to the power α, one expects a rollover energy per nucleon of

$$T_c/A \propto t^{2/(\alpha+1)}(Q/A)^{2\alpha/(\alpha+1)} \tag{4.1}$$

as a function of t, the time duration of shock acceleration.

References

Bieber, J. W., Clem, J., Evenson, P., Pyle, R., Ruffolo, D., & Sáiz, A. 2005, *Geophys. Res. Lett.* (submitted)

Bieber, J.W., Dröge, W., Evenson, P., Pyle, R., Ruffolo, D., Pinsook, U., Tooprakai, P., Rujiwarodom, M., Khumlumlert, T., & Krucker, S. 2002, *ApJ* 567, 622

Bieber, J.W., Evenson, P., Dröge, W., Pyle, R., Ruffolo, D., Rujiwarodom, M., Tooprakai, P., & Khumlumlert, T. 2004, *ApJ (Letters)* 601, L103

Bieber, J.W., & Matthaeus, W.H., 1997, *ApJ* 485, 897

Bryant, D.A., Cline, T.L., Desai, U.M., McDonald, F.B. 1962, *J. Geophys. Res.* 67, 4983

Cane, H.V., McGuire, R.E., & von Rosenvinge, T.T. 1986, *ApJ* 301, 448

Cliver, E.W., Kahler, S.W., & Reames, D.V. 2003, *ApJ* 605, 902

de Hoffmann, F., & Teller, E. 1950, *Phys. Rev.* 80, 692

Desai M.I., Mason, G.M., Dwyer, J.R., Mazur, J.E., Gold, R.E., Krimigis, S.M., Smith, C.W., & Skoug, R.M. 2003, *ApJ* 558, 1149

Desai, M.I., Mason, G.M., Wiedenbeck, M.E., Cohen, C.M.S., Mazur, J.E., Dwyer, J.R., Gold, R.E., Krimigis, S.M., Hu, Q., Smith, C.W., & Skoug, R.M. 2004, *ApJ* 611, 1156

Drury, L.O'C. 1983, *Rep. Prog. Phys.* 46, 973

Ellison, D.C., Ramaty, R. 1985, *ApJ* 298, 400

Evenson, P., Meyer, P., Yanagita, S., & Forrest, D.J. 1984, *ApJ* 283, 439

Forbush, S.E. 1937, *Phys. Rev.* 51, 1108

Giacalone, J., & Jokipii, J.R., 1999, *ApJ* 520, 204

Gosling, J.T., Asbridge, J.R., Bame, S.J., Feldman, W.C., Zwickl, R.D., Paschmann, G., Sckopke, N., & Hynds, R.J. 1981, *J. Geophys. Res.* 86, 547

Hsieh, K.C., & Simpson, J.A. 1970, *ApJ (Letters)* 162, L191

Hurford, G.J., Mewaldt, R.A., Stone, E.C. & Vogt, R.E. 1975, *ApJ (Letters)* 201, L95

Jokipii, J.R. 1966, *ApJ* 146, 480

Klecker, B., Hovestadt, D., Gloeckler, G., Ipavich, F.M., Scholer, M., Fan, C.Y., & Fisk, L.A. 1984, *ApJ* 281, 458

Klecker, B., Scholer, M., Hovestadt, D., Gloeckler, G., & Ipavich, F.M. 1981, *ApJ* 251, 393

Lee, M.A. 1983, *J. Geophys. Res.* 88, 6109

Lee, M.A., & Ryan, J.M. 1986, *ApJ* 303, 829

Luhn, A., Klecker, B., Hovestadt, D., & Möbius, E. 1987, *ApJ* 317, 951

Mason, G.M., Gloeckler, G., & Hovestadt, D. 1984, *ApJ* 280, 902

Matthaeus, W.H., Gray, P.C., Pontius, D.H., Jr., & Bieber, J.W. 1995, *Phys. Rev. Lett.* 75, 2136

Matthaeus, W.H., Qin, G., Biebier, J.W., & Zank, G.P. 2003, *ApJ (Letters)* 590, L53

Mazur, J.E., Mason, G.M., Dwyer, J.R., Giacalone, J., Jokipii, J.R., & Stone, E.C. 2000, *ApJ (Letters)* 532, L79

McKibben, R.B., Lopate, C., & Zhang, M. 2001, *Space Sci. Rev.* 97, 257

Ng, C.K., Reames, D.V., Tylka, A.J. 1999, *Geophys. Res. Lett.* 26, 2145

Ng, C.K., & Wong, K.-Y. 1979, *Proc. 16th Internat. Cosmic Ray Conf.* 5, 252

Nutaro, T., Riyavong, S., & Ruffolo, D. 2001, *Comp. Phys. Comm.* 134, 209

Qin, G., Matthaeus, W.M., & Bieber, J.W. 2002, *ApJ (Letters)* 578, L117

Reames, D.V. 1990, *ApJ (Letters)* 358, L63

Reames, D.V. 2000, *ApJ (Letters)* 540, L111

Roelof, E.C. 1969, in: H. Ögelmann & J.R. Wayland (eds.), *Lectures in High Energy Astrophysics,* NASA SP-199 (Washington, DC: NASA), 111

Ruffolo, D. 1995, *ApJ* 442, 861

Ruffolo, D. 1997, *ApJ* (Letters) 481, L119

Ruffolo, D., & Channok, C. 2003, *Proc. 28th Internat. Cosmic Ray Conf.* 6, 3681

Ruffolo, D., Khumlumlert, T., Youngdee, W. 1998, *J. Geophys. Res.* 103, 20591

Ruffolo, D., Matthaeus, W.H., & Chuychai, P. 2003, *ApJ* (Letters) 597, L169

Ruffolo, D., Tooprakai, P., Rujiwarodom, M., Khumlumlert, T., Bieber, J.W., Evenson, P., & Pyle, R. 2004, *Eos Trans. AGU* 85, Jt. Assem. Suppl., Abstract SH31A-04

van Nes, P., Reinhard, R., Sanderson, T.R., Wenzel, K.-P., & Roelof, E.C. 1985, *J. Geophys. Res.* 90, 398

Zhang, J., Dere, K.P., Howard, R.A., & Vourlidas, A. 2004, *ApJ* 604, 420

Discussion

UNKNOWN: Comment: At the time of the 2001 April 15 event halo observations show the CME at $\sim$0.3 R$_\odot$. So if it is shock acceleration it is operating from very low heights.

RUFFOLO: Yes, I agree.

JIE ZHANG: For the two events you studied, you showed that the proton onset time is close to soft X-ray peak time. This implies that you start to see SEP at the end of CME acceleration based on my observation of CME flare relation. My question is whether the coincidence (proton onset - soft X-ray peak), is true for many other events? Any statistics on this?

RUFFOLO: We would certainly like to study more events! The analysis I showed was for data from the Spaceship Earth network of polar neutron monitors. This has only been operational, with one-minute resolution, since 2001. Thus we have only been able to analyze 3 events, the two shown here and also a small GLE on Aug. 24, For these, the proton onset is consistent with the soft X-ray peak. 2002.

SCHWENN: GeV particles accelerated near the Sun early on and MeV particles accelerated in IP space – What evidence do you have that they all came from one identical shock? There are people who think in a 2-shock scenario: 1) CME shock(driven) and 2) flare shock (blast wave), associated with Type II radio burst.

RUFFOLO: If the flare shock is delayed from the primary energy release, then we cannot rule this out based on timing alone. But let me point out that at lower ion energies, tens of MeV/n, there is strong physical evidence that the ions accelerated near the Sun came from the CME-driven shock (Mason et al, 1984, Lee & Ryan 1986, Reames 1990, Ruffolo 1997) and not from a localized source, or a source deep in the corona.

BOTHMER: There is a problem of importance: (a) Transport vs Position of the source; (b) Species: Electrons, Protons. Just a comment, not really a question.

RUFFOLO: Yes, I had actually prepared a review of these issues but I had to drop them due to a lack of time.